Aerospace Science and Technology 140 (2023) 108450

Contents lists available at ScienceDirect

Aerospace Science and Technology

journal homepage: www.elsevier.com/locate/aescte

Fuel sloshing-induced effects on the dynamic response of a scaled research wing demonstrator

Lucian Constantin [a,b,*], Joe J. De Courcy [b], Brano Titurus [b], Thomas C.S. Rendall [b], Jonathan E. Cooper [b]

[a] SATAS Centre of Excellence, Military Technical Academy "Ferdinand I", Bucharest, Romania
[b] Department of Aerospace Engineering, University of Bristol, Bristol, United Kingdom

ARTICLE INFO

Article history:
Received 14 February 2023
Received in revised form 26 May 2023
Accepted 7 June 2023
Available online 13 June 2023
Communicated by Marwan Al-Haik

Keywords:
Fuel sloshing
Damping
Wing dynamics
Scaled wing
Vibration testing

ABSTRACT

Fuel sloshing inside aircraft wing tanks is not currently considered as a means of passive loads alleviation due to the lack of maturity of modelling tools and overall understanding of vertical sloshing. In this work, a scaled research wing demonstrator is presented, designed for the study of fuel sloshing inside an aircraft wing-representative model. An experimental campaign was conducted to examine the impact of fuel sloshing on the vertical dynamics of a scaled aircraft wing demonstrator, investigating the influence of excitation amplitude, filling level, baffle geometry, spanwise liquid position, and dihedral angle. It was found that the sloshing of the liquid in the fuel tank causes significant energy dissipation following step release excitation, maximized in the 40-60% filling range depending on the dihedral angle. The sloshing-induced damping also varies with the amplitude of excitation, with maximum added damping ratio of 0.038 achieved earlier in the motion at larger excitation amplitudes. The spanwise distribution of the liquid was found to have the strongest effect on the sloshing-induced damping, with the baffles' main impact being through the compartmentalization of the tank. Solid baffles that maintain favorable liquid distribution can increase the damping effect, while perforated baffles are not as effective. This work indicates that by considering the fuel dynamics rather than the fuel equivalent dry mass during the aircraft wing design, the net damping may be increased, leading to lighter wing structure designs.
© 2023 The Author(s). Published by Elsevier Masson SAS. This is an open access article under the CC BY license (http://creativecommons.org/licenses/by/4.0/).

1. Introduction

A commercial aircraft stores most of the fuel inside its integral wing tanks and in the fuselage between the wings. Unlike pylon-mounted tanks located on the wing exterior, *integral* tanks are fully or partially constituted by the wing structure itself. Typically, the fuselage space is reserved for passengers and cargo and larger aeroplanes can use the tail and empennage for extra fuel storage (e.g. the Airbus A380-800 is equipped with the fuel tanks inside its horizontal stabilizer [1]). Such fuel storage architecture opens up an often overlooked possibility of passive means of loads alleviation and increased effective wing damping, through exploitation of the dynamic interaction between the wings and fuel inside their integrated tanks. It is in this context within which the sloshing-induced damping was investigated in the EU-funded Airbus-led *"SLOWD"* (SLOshing Wing Dynamics) project [2]. One of its aims was to investigate the feasibility of using fuel sloshing induced damping as a means of reducing the design loads in large passenger aircraft. Currently, in the European Union, such aircraft fall under the regulatory requirements of the European Union Aviation Safety Agency (EASA) CS-25 Acceptable Means of Compliance (AMC) [3] which, in relation to the modelled damping, stipulates: "*In the absence of better information it will normally be acceptable to assume 0.03 (i.e. 1.5% equivalent critical viscous damping) for all flexible modes. Structural damping may be increased over the 0.03 value to be consistent with the high structural response levels caused by extreme gust intensity, provided justification is given.*" [3].

Classically, fuel sloshing is not taken into account during the aircraft design phase and only an equivalent solid mass of the liquid is considered. However, an earlier pre-SLOWD work indicated that liquid sloshing in vertically vibrating wing-like systems can increase the effective damping. Titurus et al. [4] and Gambioli et al. [5] described a sloshing beam experiment that was representative of certain structural and dynamic wing bending characteristics as well as its fuel tank design. It was observed experimentally that significant damping was induced in the system with freely sloshing liquid and the main damping trends were outlined. These preliminary studies thus showed that fuel sloshing introduces hy-

* Corresponding author.
E-mail address: lucian.constantin@mta.ro (L. Constantin).

https://doi.org/10.1016/j.ast.2023.108450
1270-9638/© 2023 The Author(s). Published by Elsevier Masson SAS. This is an open access article under the CC BY license (http://creativecommons.org/licenses/by/4.0/).

drodynamic loads which depend on wide range of parameters and operational conditions, an important aspect that will be experimentally investigated in this work.

Recent research has mainly focused on spacecraft and satellite sloshing problems using analytical [6] as well as experimental [7] methods. The present research aims to achieve improved understanding and characterisation of the experimentally observed sloshing dissipative effects experienced in a novel demonstrator representing a wing-like structure during strong out-of-plane vibrations. Prior to this work, sloshing-induced damping due to vertical liquid sloshing was systematically studied in [8], where the variation of damping with the filling level and excitation amplitude in a single degree of freedom vibrating setup was demonstrated. Further, the in-depth characterisation of sloshing-induced hysteresis cycles and the analysis of the damping saturation phenomenon was explored in [9–11]. Finally, supplementary numerical investigations were also considered within the SLOWD scope and linked with the development of reduced order models [12,13].

In the broader research context, early liquid sloshing research in aircraft fuel tanks dates back to the 1940s. Increasing in their size, some aeroplanes would now carry fuel with a mass comparable to the empty mass of the structure [14]. In certain instances, the pilots began to observe the fuel sloshing effects and their impact on the aircraft stability. Focusing on aircraft stability and manoeuvrability, the fuel sloshing problem was first studied by the National Advisory Committee for Aeronautics (NACA U.S.) and the Douglas Aircraft Company, Inc., starting in 1949. Empirical solutions such as baffles were explored, with pilots reporting substantial mitigation of the sloshing-induced dynamics when the tanks were equipped with baffles.

The first systematic studies were carried out by Smith [14], who built an experimental aircraft model with two large spherical, unbaffled, fuel tanks attached, and investigated the aircraft stability. In these initial studies the frequencies of oscillation between the structure and the liquid were not matched, so a worst-case scenario was not reached. However, effects were noticed where sloshing motions induced high-frequency “jerky” motions modulated over the lateral motions of the aircraft. The sloshing effects were also found to be dependent on the liquid mass-to-structure ratio and its moment of inertia. From a numerical modelling perspective, building upon these experimental results, Graham [15,16] showed for the first time that simple pendula responses could be made consistent with the small amplitude fuel sloshing and resulting loading, paving the way towards equivalent mechanical modelling of sloshing forces. In [16], Graham also mentioned the possible effects of varying the effective centre of gravity, this introducing parametric sloshing, with possible implications in missile dynamics and aircraft manoeuvres. Schy [17] introduced the first analytical treatment of the theory of sloshing, for the spherical tank case. He foresaw possible future directions of study involving higher amplitude sloshing which proved to be fruitful, indicating that larger amplitude sloshing regimes may lead to more stable aircraft oscillations since energy is lost through splashing. Luskin [18] then extended the previous work and showed analytical arguments that sloshing can be mitigated using baffles. This work conducted at the end of the 1940s represents the basis for the much interest that followed regarding aircraft and missile stability, as well as the use of baffles to dampen fuel sloshing.

Following these early studies, limited research was conducted on induced damping and flutter effects as well. Merten and Stephenson’s [19] were the first to study the effect of fuel sloshing on a vibrating beam under step release excitation, with a tank attached at the tip of the beam. Considering that this was the first study of such a system, many useful conclusions were reached experimentally. The authors used two models with different liquid-to-structure mass ratios, as well as different filling levels and liquids. They reached the following conclusions for the particular beam sloshing systems that they had studied: (1) damping was maximized and was approximately constant in the 30-50% filling level range; (2) dissipative sloshing energy reached a maximum in the second or third oscillation cycle, showing little dissipation in the first cycle; (3) damping was found to be highly dependent on liquid density while viscosity had no noticeable effect. While these are very useful and relevant results, the tests were conducted on simplified beam structures with tip tanks rather than the more standard configurations with wing-integrated fuel tanks. Follow on research shifted towards the quantification of effective mass and inertia of the fluid, with applications in flutter analysis. In this context, further work at NACA [20,21] investigated the pitching excitation of multiple sloshing tanks. Baffled and unbaffled cases were considered, with different pylon mounting configurations. The effective mass of the sloshing liquid inside wing-supported tanks was seen as potentially having an influence on flutter characteristics. Flutter systems with pylon-mounted fuel tanks, either simplified two-degrees freedom systems [22,23] or realistic models [24], were studied as well. It was found that the *effective* rather than dry inertia of the fuel must be taken into account in the study of flutter, the two giving very different predictions. There was also experimental indication that for bending-to-torsion frequency ratios in the vicinity of unity, additional liquid damping increases the flutter speed and, if the flutter phenomenon builds up slowly enough such that liquid starts sloshing violently, flutter amplitude may be limited. Sewall [23] demonstrated a chordwise fuel emptying sequence for both integrated and pylon-attached fuel tanks that maximizes flutter speed. Further research then focused on the influence of liquid inertia on flutter rather than sloshing-induced damping [24–26].

Valuable as these results are, the technical capabilities of the 1940-1950s era were limited in both experimental and numerical investigations. Even though it was observed that substantial, violent liquid movement that depended on oscillation amplitude occurs, the depth of the experimental analysis was limited and moreover, there were no analytical and numerical tools available at that time to further the investigations. Focus was placed on external tanks which were common for aircraft of that time, although they are substantially different from the contemporary integral wing fuel tanks in the liquid distribution as well as tank geometry. Outside of the SLOWD project and limiting the scope to aerospace applications, with the emergence of prospective novel fuels and aircraft architectures, fuel sloshing in aircraft wings gains, yet again, increasing research attention with examples mostly in the numerical modelling of the influence of lower amplitude lateral sloshing on flutter margins [27–29].

Based on the body of work presented previously, the aim of this paper is to analyze experimentally the effect of fuel sloshing and its effect on the dynamic response of a novel aircraft wing-fuel tank research demonstrator. The objectives are to investigate the influence of the main parameters of the wing and spatially distributed fuel tank on the sloshing-induced dynamics effects, namely: the effect of excitation amplitude, spanwise liquid position, filling level, baffle geometry and dihedral angle. In order to introduce the research, the paper is organized as follows. Section 2 outlines the research methodology and main tools of analysis, as well as the experimental setup that was used for this research. Section 3 presents the experimental results and analysis. Conclusions are drawn in Section 4.

2. Methodology

To enable focused and systematic fuel-sloshing research in the context of controlled and repeatable experiments, a Froude-scaled research wing demonstrator [30] was developed based on the full

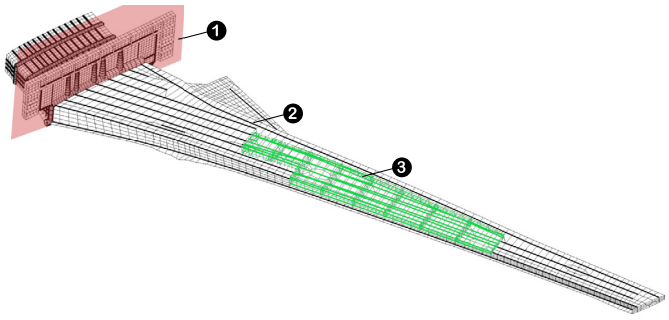


Fig. 1. Full-scale wingbox model. (1) – Shear wall/ encastre condition, (2) – Wingbox, (3) – Main fuel tank.

scale wing-box model of the modern single-aisle airliner wing [13]. This section is dedicated to the introduction of this novel demonstrator as well as the description of the testing methodology.

2.1. Scaled research prototype model

This research aims to investigate fluid-structure interaction and sloshing phenomena across a wide range of conditions which include highly nonlinear impact sloshing and breaking waves. The demonstrator design is thus influenced by this key requirement. The scaling of sloshing loads when impacting phenomena are present has received particular attention in the Liquefied Natural Gas (LNG) transportation industry, with Bass et al. [31] emphasizing that Froude similarity ($Fr = \sqrt{a/g}$, where a is a vertical acceleration and g is the gravitational acceleration) is required to reproduce the impacting sloshing conditions.

Froude similarity and the reference research wingbox model shown in Fig. 1 were thus used to design the demonstrator. A detailed discussion of this process is provided in [30]. The demonstrator is equipped with a shear wall that emulates the effect of the fuselage on the wing structure. For the purposes of this work, it is considered the encastre (cantilever) plane. A large integral fuel tank is located inside the wingbox structure. The wingbox out-board of the shear wall plane (1) and the fuel tank (3) were scaled down by the geometrical factor 1:5. Since it would lead to impractical design and material requirements, it was not possible to scale down the wingbox directly while conserving all geometry properties. Instead, an equivalent design consisting of the two spars and multiple torque tubes [32], scaled to stiffness and dynamic characteristics, was adopted. The wingbox was condensed into the leading and trailing edge spars that provide the bending stiffness and multiple torque tubes that confer its torsional stiffness. The added fuel tank partly contributed to the stiffness of the demonstrator and increasing its overall complexity. The details of the scaling procedure, assumptions and main results can be found in [30]. Due to the use of proprietary and confidential information when designing the demonstrator, selected quantities shown in this work (e.g., the modal frequencies of the scaled model) are normalized.

Fig. 2 shows the assembled scaled demonstrator and the test instrumentation. The challenging functional requirements imposed numerous design constraints. An example of these is the decision to place a discrete fuel tank subassembly on top of the main structure to enable observability of the liquid sloshing. The main subassemblies are numbered as follows: the structure is cantilevered to the wall using the root connection (1); the main wing structure is shown in (2), with the scaled fuel tank placed on its top (3) and, finally, the loading points and associated mechanism is shown in (4).

Fig. 3 shows a detail of the fuel tank, manufactured from Tufnol (base and side pillars), polycarbonate (side walls) and acrylic (baf-

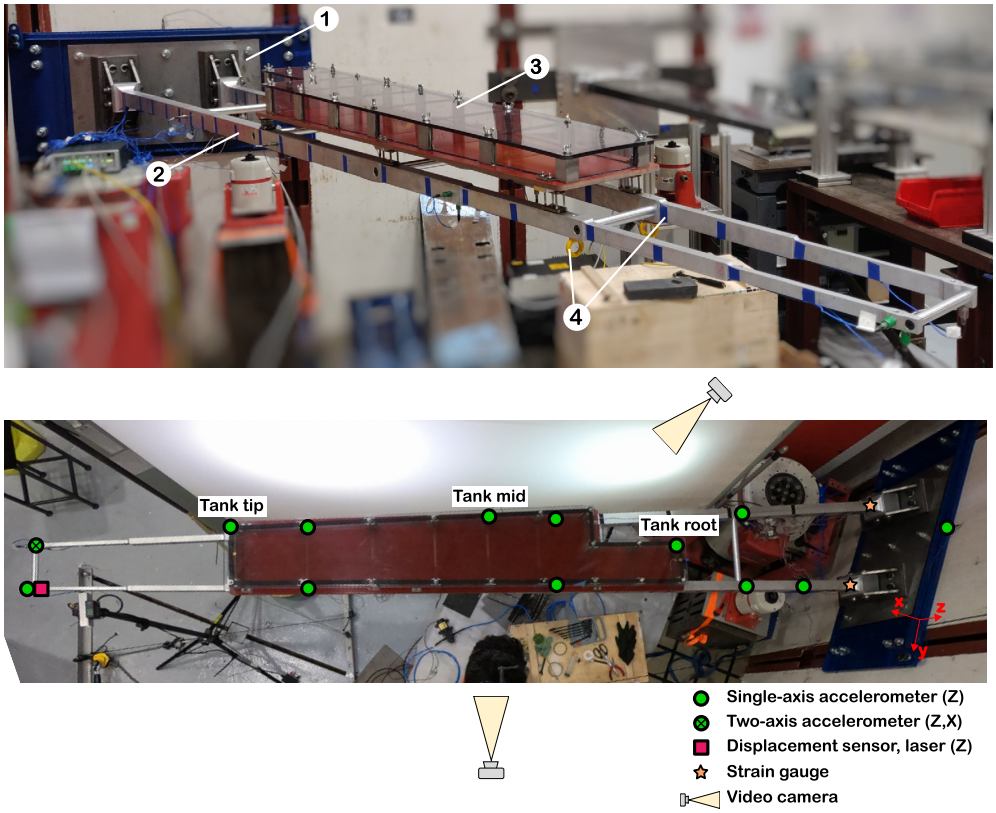
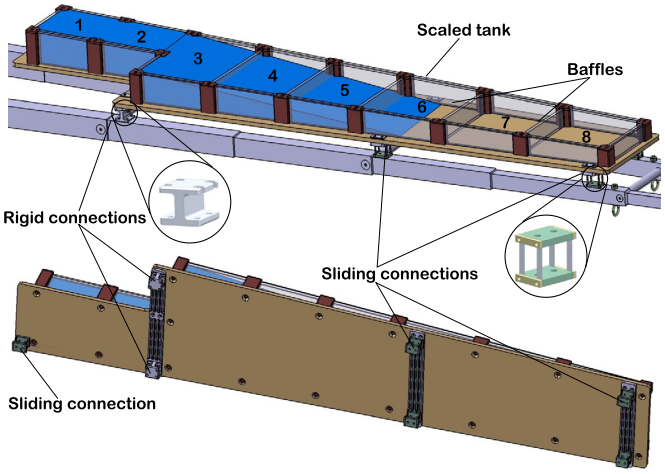
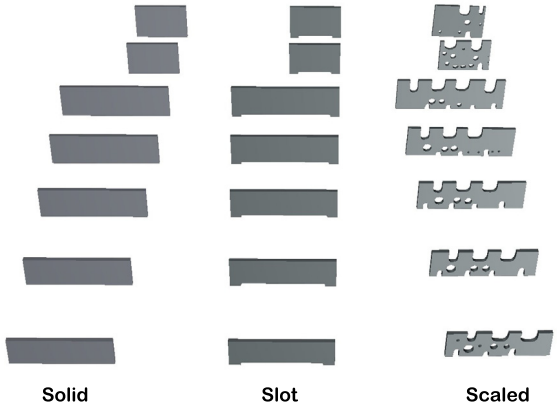


Fig. 2. Scaled test specimen. Top figure: (1) – Cantilever to the strong wall connection, (2) – Scaled structure model, (3) – Scaled fuel tank model and (4) – Loading points for step release tests. Bottom figure: Instrumentation layout. (For interpretation of the colours in the figure(s), the reader is referred to the web version of this article.)



(a) Fuel tank and connections to the underlying structure. Removable baffles split the tank into 8 isolated or interconnected cells.



(b) Baffles used for the scaled tank compartmentalization

Fig. 3. Scaled fuel tank and baffle details.

fles). It is divided in 8 cells with the removable baffles. To enable analysis of the liquid sloshing patterns, the most challenging requirement to be met was the observability of the liquid inside the tank from multiple directions. This constraint resulted in the positioning of the scaled tank on top of the main structure, which in turn also led to the necessity of connecting the fuel tank to the underlying structure without introducing added parasitic effects such as excessive reaction loads, friction, freeplay or other sources of uncertainty and unwanted energy dissipation. As can be seen in Fig. 1 and 2, the tank spans a considerable length of the structure (approximately 50%). If the tank subassembly was rigidly connected to the main structure, on the one hand, the main structure would be excessively stiffened in the tank region and, on the other hand, the tank's constituent components would have to transfer and withstand excessive internal loads. Consequently, to reduce the load transfer between these two crucial but functionally different subsystems and to minimise the local stiffening effect, a novel interface design consisting of two relatively rigid connection points and five flexure connections realising nearly free tangential sliding was proposed and implemented between the tank and the underlying main structure, as shown in Fig. 3a. The baffles in the fuel tank are removable and replaceable, and the types of baffles that were investigated are shown in Fig. 3b. The "solid" baffles had a solid surface and the foam gasket was used to seal each tank cell individually. For the wet tests with solid baffles, each tank cell was filled to its own individual filling level, representing fractions of the volumes shown in Table 1.

Table 1
Fuel tank cells volumes.

Cell no.	1	2	3	4	5	6	7	8
Volume [L]	1.71	1.66	3.22	2.90	2.53	2.43	2.05	1.70
Total [L]	18.2							

The "slot" baffles have a 5 mm slot at their bottom, allowing the liquid to flow between cells under quasi-static conditions, e.g. when the wing sits still or when it is being loaded for step release. It is shown later that these slots generally block the flow under the dynamic test conditions (across the short time scales), i.e. following the step release. This slot baffle configuration is studied and contrasted against the case without the baffles in order to assess the influence of the spanwise flow on the sloshing-induced effects. Finally, the "scaled" baffles are representative of an airliner's baffles with a more complex internal geometry and are directly scaled from the reference wingbox structure.

2.2. Test methodology

Multiple sets of experiments were performed in order to evaluate systematically the effect of liquid sloshing on the test structure's dynamic response under different parametric variations. The tests may be categorized as low and high amplitude cases, where the low-amplitude tests were performed to evaluate the modal behaviour of the structure, whilst the high-amplitude ones were conducted to assess the liquid sloshing effects.

For the high-amplitude wing behaviour, there are different types of input considered during the aircraft certification, such as discrete or continuous gusts [3]. Among these, the two main discrete gust models, illustrated in Fig. 4, are: (a) the sharp-edged gust and (b) the 1-cosine gust [33]. The sharp-edged gust models the *uniform* atmospheric vertical velocity field $\dot{z}_w$ which starts and ends abruptly [34]. Being considered more realistic, the 1-cosine gust model is currently being used for aircraft certification [3]. Principally, in each case, there is a time t_0 where the aircraft encounters the gust velocity field $\dot{z}_w$, and a time when it peaks, named here "release" time t_r and after the gust ends, the structure vibrates freely in assumed steady air flow. The typical wing dynamic response is shown underneath the models as well in Fig. 4. Note that while the two scenarios (gust models and step release) are not identical and are prescribed using velocity and displacement fields respectively, the free-decay dynamic response will be similar.

Owing to their practical significance, the high-amplitude gust-induced responses represent extreme conditions which the combined fuel-wing system experiences during its operation. While the frequency characteristics of the specific gust response depend on numerous factors [35], where the gust gradient (duration) can be seen as the major influence, the first or fundamental mode generally retains its strongly dominant role. Repeatable test conditions where such characteristics can be readily attained are those that follow after *step-release excitation*. Merten and Stephenson [19] originally applied this method to generate large-amplitude free-response conditions in the case of two cantilevered beams with partially filled tanks attached to their tips. A similar approach was used to study the full-scale wingbox structure damping in [36] and later to study fluid-structure interaction in a wing-like beam structure, [4,5].

As shown in Fig. 4 (c), during this type of test the structure is loaded quasi-statically up to a pre-defined vertical displacement z_w, reaching the structural deformations comparable to those induced by the gust loading. Since the liquid sloshing behaviour is of interest in this work, the quasi-static loading conditions are necessary in order to not disturb the liquid inside the tank, and may be

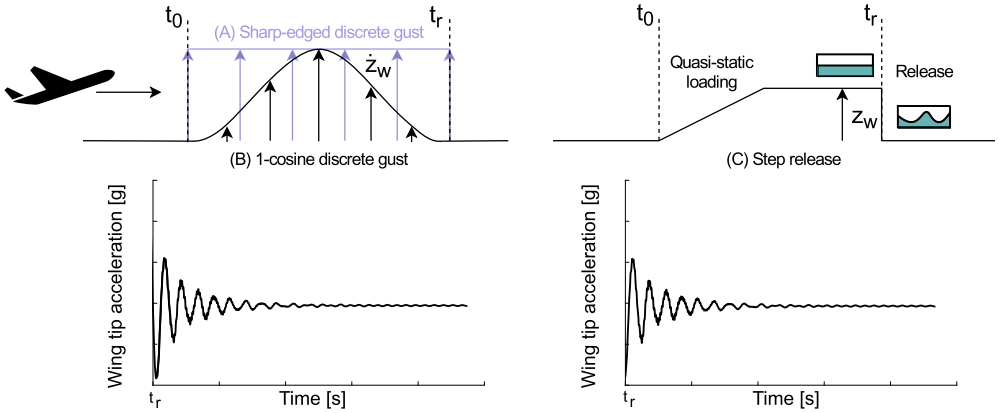


Fig. 4. Discrete gust models and step release excitation. Characteristic wing dynamic response shown underneath each model.

Table 2
Test matrix for the scaled model experimental campaign.

Test no.	Repetitions	Test type	Fill [%]	Added mass [%]	Λ [°]	Baffles
D1-2	6	GVT/burst random	0	0	0	No, solid
D3-5	10	GVT/burst random	0	0	6.9	No, slot, scaled
D6-14	10	GVT/impact hammer	0	0	6.9	No
D15-26[a]	1	Step release	0	0	0	No
D27-29	3	Step release	0	30,50,70	0	No
D30-31	3	Step release	0	0	6.9	No, slot
W1-2	3	Step release	30	0	0	No, slot
W3-4	3	Step release	70	0	0	No, slot
W5-7[a]	3	Step release	50	0	0	Solid
W8-12	3	Step release	30-70	0	0	Solid
W13-15[b]	3	Step release	30	30	0	No
W16-18[b]	3	Step release	50	50	0	No
W19-21[b]	3	Step release	70	70	0	No
W22-24	3	Step release	30	0	6.9	No, slot
W25-26	3	Step release	50	0	6.9	No, slot
W27-28	7	Step release	70	0	6.9	No, slot
W29-37	3	Step release	10-90	0	6.9	Scaled

[a] Tests at multiple initial amplitudes.
[b] Tests at selected spanwise locations.

achieved by loading the structure slowly. The structure can then be released nearly instantaneously at time t_r from the deflected position z_w, after which it vibrates freely in a similar fashion to the dynamic response following a gust encounter.

To complement the step-release tests that are likely to feature significant structure and fluid-structure born nonlinear effects, the standard ground vibration tests (GVT) were conducted at low amplitudes using burst random excitation with the electrodynamic shaker (model LDS V406), complemented with tap-testing using the impact hammer (model PCB 086C01). Both sets of tests were conducted in order to estimate the modal properties of the structure in different configurations. Three of the dry tests (D27-D29) were conducted with added "frozen" mass equal to the equivalent filling level and are shown as a percentage of the equivalent tank fill. Multiple initial amplitudes were also investigated (D15-26) to ensure that it does not influence the dry damping. Two dihedral angles Λ were investigated by changing the cantilevered root connection wedges, $\Lambda = 0°$ and $\Lambda = 6.9°$, the latter being the same as the full-scale wingbox model and thus representative of a typical airliner wing.

The wet tests were conducted at the room temperature with tap water as the working liquid, with and without trace amounts of dye to improve the observation of the sloshing patterns. Previous studies have found that vertical violent sloshing is not sensitive to the liquid viscosity except for extremely low viscosities [37]. Therefore, tap water was considered a good substitute for aircraft fuel under these investigations. The main varied parameters in the wet case were the filling level (10% to 90% with 10% increments), baffle type, dihedral angle and spanwise position of the liquid. Tests W13-W21 (marked with a star in Table 2) were conducted for different spanwise positions of the liquid. In this latter case, the solid baffles were used to seal and fill the different sections of the tank selectively for each filling level, as follows (using the tank cell numbering in Fig. 3): cells 1-3, 4-5 and 6-8. Depending on the selective filling level case, equivalent frozen mass was added inside all other cells. More details on this approach to divide the tank into various working sections will be given later in results.

3. Results and discussion

To gain the understanding of the reference behaviour of the system in the absence of sloshing, initially, the experimental results are presented with the focus on the system without the liquid (dry tests/system). The focus will then be shifted to the system with the liquid inside the fuel tanks (wet tests/system), evaluating the influence of excitation amplitude, spanwise liquid position, baffles and dihedral angle.

3.1. Experiments without liquid

Multiple experimental modal analysis (EMA) tests were performed on the scaled structure, before and after changing the root wedges (dihedral angle) in order to make sure that the system properties were not significantly affected by the change in

Table 3
Demonstrator modal properties.

Mode #	F	ζ [%]	Mode shape	MCF
1	F_1	0.06	1^{st} bending	1.67%
2	$4.85F_1$	0.32	2^{nd} bending	0.01%
3	$5.65F_1$	0.43	1^{st} torsion + bending	0.07%
4	$6.57F_1$	0.46	1^{st} torsion	0.05%
5	$10.41F_1$	0.39	3^{rd} bending	0.01%
6	$13.88F_1$	1.32	2^{nd} torsion	1.41%
7	$16.38F_1$	0.81	4^{th} bending	0.15%

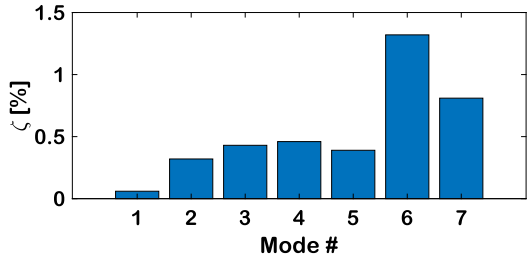


Fig. 5. Demonstrator modal damping bar chart.

the root conditions. In terms of modal identification, tests D6-D14 were the most comprehensive from the point of view of the number of test repetitions and number of observed points. The tank was excited using the modal hammer at the eight different locations distributed across the leading and trailing edge and the response was recorded at all acceleration measurement stations. The data were collected using the Siemens LMS system with 16 input channels and processed using Siemens TestLab and Matlab. The PolyMAX system identification method [38] was used to estimate the modal parameters (frequency, damping and mode shape) of the structure.

The summary of the EMA tests is shown in Table 3 and Fig. 5, showing the frequency of each mode in terms of the first bending component F_1, the damping ratio, a description of the mode shape and the mode complexity factor (MCF). The modal damping values are also shown in the bar chart in Fig. 5, for easier comparison between the different modes; the first bending mode is especially lightly damped.

Note that the damping and frequency results shown thus far are representative only for the low amplitude vibrations of the structure. Due to the dry structural nonlinearities, the high-amplitude values will differ and will be introduced next together with the wet results for ease of understanding. The presented values, in particular F_1, can be used as a reference during the subsequent high-amplitude experiments. The increased values of modal damping at the second and subsequent modes are attributed to more pronounced engagement of the interfaces and joints present within the assembled demonstrator.

3.2. Experiments with liquid-filled tanks

In this section, the experimental cases with liquid inside the tank are considered. A detailed analysis of only one filling level for all frequency components was already presented in [39], where it was shown that, for the type of excitation considered in this work, the liquid sloshing has no significant influence on the higher frequency vibration components, but it does have a significant effect on the first out-of-plane bending mode. Focus will thus be placed in this section on the influence of sloshing on the first bending mode only.

3.2.1. Characteristic response

Fig. 6 shows an initial representation of the fuel tank tip acceleration with respect to time (accelerometer "tank tip" in Fig. 2), dry versus 50% filling level with solid baffles, in order to emphasize the main qualitative characteristics of the demonstrator's dynamic response. According to Table 2, multiple tests were conducted for each configuration.

Here, the repetitions were averaged and, in Fig. 6, the mean values are shown with green and gray bands indicating the maximum and minimum variation around the mean. The time axis was normalized using the first out-of-plane bending period of oscillation. There are multiple features that become apparent when studying the characteristic dynamic response of the structure with liquid compared to the dry case. First of all, indicated by the narrow error bands, very good repeatability is observed among the repetitions for both dry and wet cases. In both cases there is a richer frequency content immediately after the step release, since the step excitation introduces energy into multiple modes of vibration. The higher frequency components, however, are excited less and also

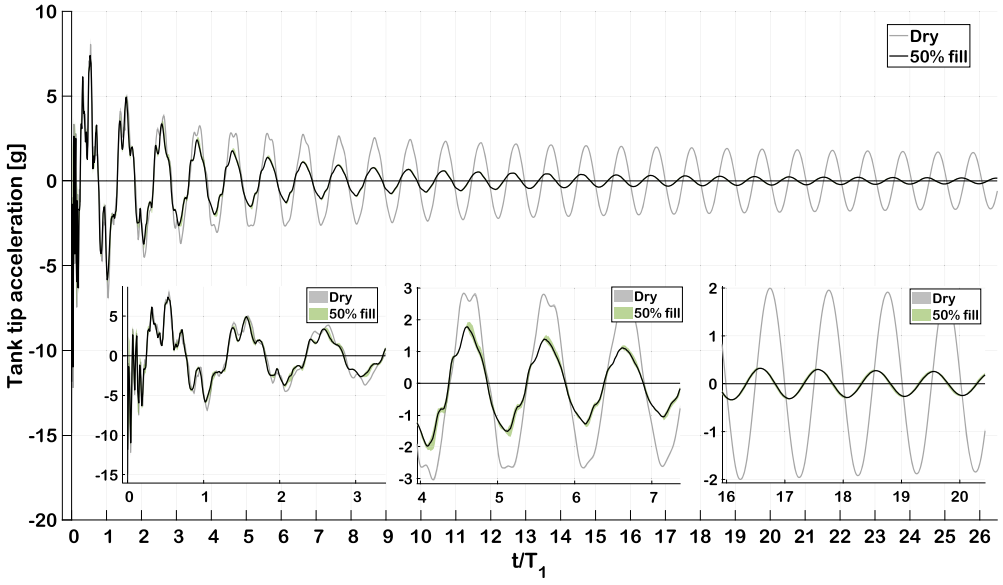


Fig. 6. Typical sloshing response of the test structure, 50% filling level case compared to the dynamically equivalent dry case.

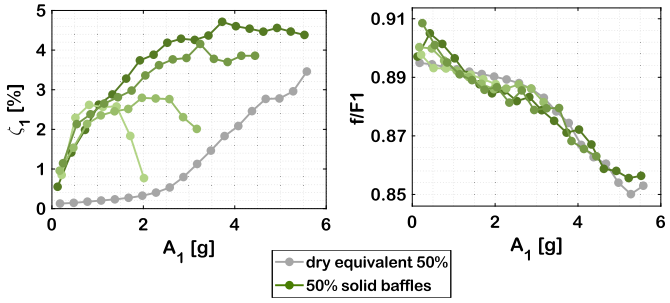


Fig. 7. Damping ratio and frequency versus amplitude for multiple initial deflections.

damped at various rates, which were shown to be largely independent of the presence of the liquid inside the tank [39]. However, the participation and vibration of the first bending mode persists for longer while its amplitude drops fast in the 50% fill case due to the sloshing action of the liquid.

Due to structural and liquid-induced nonlinearities at the large amplitude excitation however, the identified frequencies and damping values are not constants and they change with the excitation amplitude. In order to characterise the nonlinear variation of these quantities with respect to the amplitude of excitation, the raw acceleration response is decomposed into the constituent frequency components using the nonlinear least-squares (NLS) identification technique described in [39].

3.2.2. *Effect of excitation amplitude*

Before investigating the influence of other parameters such as filling level or spanwise liquid distribution, we first assess the influence of the initial deflection on the fuel sloshing-induced damping. Most of the sloshing tests presented in this chapter are step release tests from one initial deflection of 2.7% semispan at the tip of the wing. It is chosen to excite all expected vertical sloshing regimes [8] (R1 – violent vertical motion caused by large vertical amplitudes of excitation, R2 – motion dominated by one sloshing mode, and R3 – small structural vibrations with minimal sloshing contribution) whilst not posing any risk to the structure's integrity. Some tests (W5-W7) were performed from the different initial amplitudes. The demonstrator configuration considered for the initial amplitude variation study is the one with the solid baffles, 0° dihedral angle and 50% filling level case.

Fig. 7 shows the damping ratio (ζ_1) and frequency (f), normalized to the first bending mode frequency, versus the acceleration amplitude (A_1) for the first bending component for four initial deflections. The frozen mass case is shown as well for comparison, and the average initial acceleration varies between 2g and 6g. Each data point is an averaged damping or frequency value obtained after applying the NLS identification algorithm [39] and averaging among the repetitions.

Following the step release event, the structure vibrates mainly vertically, which causes the liquid inside the tank to start sloshing. Fig. 7 indicates that, depending on the initial amplitude, there is variability in the damping ratios in the first part of the transient decay. As already pointed out in [19], the explanation for this phenomenon lies in the fact that following the release event, the sloshing takes time to develop. Here, it can also be observed that the time for the sloshing to develop generally decreases with the increasing excitation amplitude.

To highlight this observation further, Fig. 8 shows three snapshots of the sloshing tank at the end of the first period of motion for the three different initial deflections (indicated here by the maximum A_1 accelerations) representative of the three cases shown in Fig. 7. For the lowest amplitude case, because of the relatively small vertical accelerations, it takes multiple periods of motion for the liquid to develop its sloshing activity and consequently, the damping ratio is almost equal to the dry structure's ratio in the first part of the transient. As the initial wing tip deflection increases, the vertical sloshing develops faster and in multiple tank cells, due to the local increase of acceleration at each spanwise station. However, once the initial stage is over and the sloshing is fully developed, the induced damping effects follow the same evolution regardless of the initial excitation amplitude, as can be seen in the overlap of the damping curves in Fig. 7 for the intermediate acceleration levels. The frequency variation with amplitude, seen on the right-hand side of Fig. 7, is broadly insensitive to the changes in the initial amplitude and does not show a significant difference from the frozen mass case. The similar frequency trends, in turn, imply that no significant frequency effects are introduced by the sloshing liquid when varying only the initial deflection.

These observations, based on the initial sloshing development, also correlate well with previously observed trends in the transient single degree of freedom (1DOF) experiments presented in [8]. The initial sloshing development region at the first part of the transient must be kept in mind when considering lower amplitude tests especially, since the R1 regime does not occur immediately, but is less significant at large amplitudes of excitation. It is further noteworthy that, in the context of gust loads alleviation, not even the conventional active feedback-based GLA systems are effective against the first oscillation cycle loads [40].

3.2.3. *Effect of the spanwise liquid position*

The moment arm of the sloshing force with respect to the root increases when the liquid is placed further outboard. Similarly, the local vertical accelerations increase towards the tip of the wing with the F_1-dominated response. Depending on the spanwise location of the liquid, it is thus reasonable to expect different induced dynamic effects of the fluid on the structure due to its sloshing.

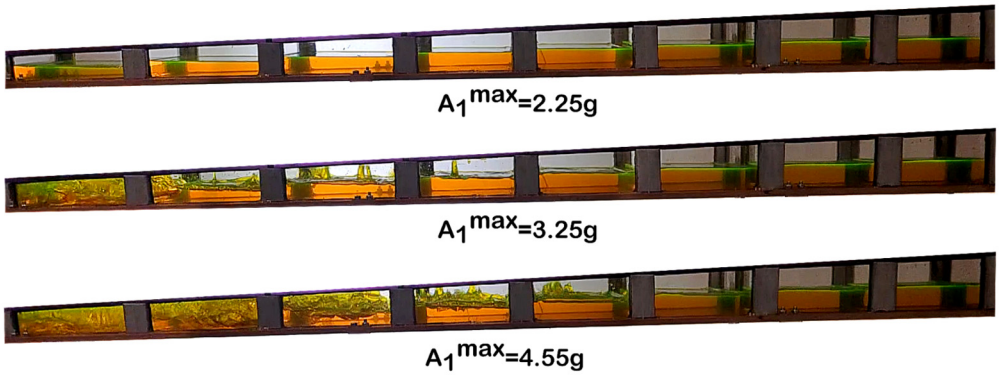


Fig. 8. Representative lateral snapshots of the sloshing tank at $t = T_1$ for different initial accelerations A_1 at the tip of the tank, 50% filling level with solid baffles.

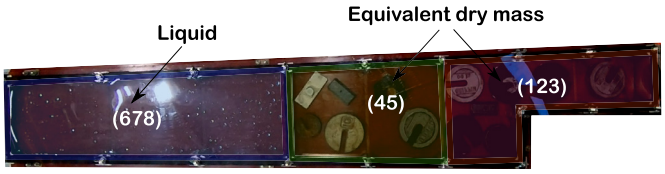


Fig. 9. Example of selective filling. Cells (678) filled and equivalent added mass elsewhere.

Table 4
Volume fractions in each cell group.

Cell group	123	45	678
% of total volume	36%	30%	34%

However, it is hard to discern the specific parameter effects when the liquid is distributed across the entire span of the tank. Generally, the fuel distribution inside wing tanks will depend on the aircraft attitude and wing deformation, unless special measures are taken to move the liquid to specific locations, which is not uncommon. For instance, for most aircraft the fuel is used to reduce the wing bending stresses by transferring it towards the wing's outer tanks after take-off, which are kept full until the end of the cruise phase. Fuel placement is also used as a means of active longitudinal centre of gravity (CG) control, maintaining the balance between the aircraft CG and the centre of lift as fuel is consumed. Another example is Concorde, where a flight engineer would be in charge of the fuel management during flight, transferring the fuel fore or aft of the aircraft tanks depending on the flight speed, as the centre of lift would change its position substantially between subsonic and supersonic regimes [41].

In order to study the effect of the liquid spanwise distribution, the tank is divided into three sections: cells 1,2 and 3 form the inboard section, 4 and 5 the middle tank section, and 6,7 and 8 the outboard one. The solid baffles are used to seal each section and in the dry sections of the tank the mass-matched solid parts are added in order to keep the mass distribution approximately constant as the liquid is transferred between the three sections. Fig. 9 shows the division of the tank in the three sections, where cells 678 are filled and equivalent dry mass is added elsewhere. Table 4 shows the distribution of the tank volume between the three sections. While the division is not perfectly equal, it is the closest possible given the existing tank cell configuration. No baffles were used in the interior of the cell groups.

Each cell group was filled during three separate tests with 30%, 50% and 70% of their volume with water, and the equivalent dry mass was added elsewhere depending on the respective filling level. As before, the structure was pulled down, then released, and the structural response was measured and processed to obtain the acceleration amplitudes, damping ratios and frequencies. Two complementary ways of the spanwise distribution effects are adopted - varying the spanwise liquid location at a set filling level and varying the filling level at set spanwise locations.

Starting with the study varying the spanwise liquid location at a set filling level, Figs. 10 to 12 show the damping ratio and frequency versus amplitude for different spanwise positions at the same filling level. There are consistent damping trends that can be observed regardless of the filling level. At the root section, cell group 123, following the step release the sloshing develops into the combined R2-R1 regime with the intermittent tank ceiling impacts. This unsteady and slowly developing behaviour lasts a relatively large number of cycles (10 cycles on average), by which time the structural damping reduces the tank tip acceleration to below 3g.

During the remaining part of the structural response, the observed damping levels are comparable to the dry case (blue versus

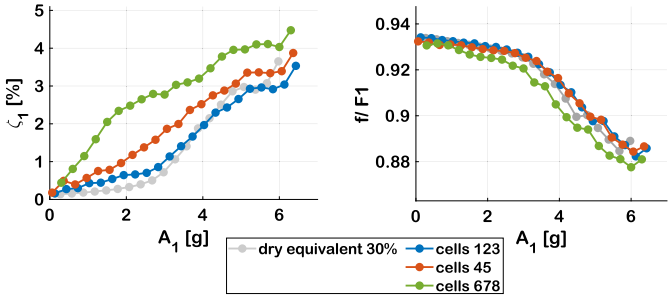


Fig. 10. Damping ratio and frequency versus amplitude for different spanwise positions at 30% filling level.

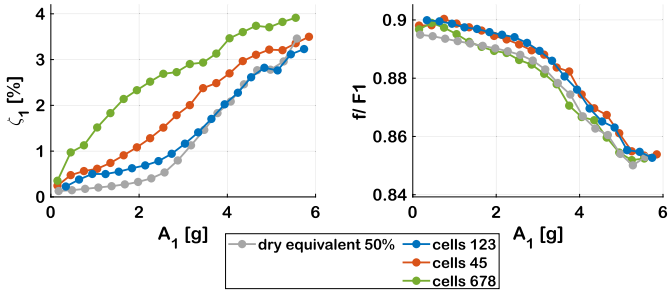


Fig. 11. Damping ratio and frequency versus amplitude for different spanwise positions at 50% filling level.

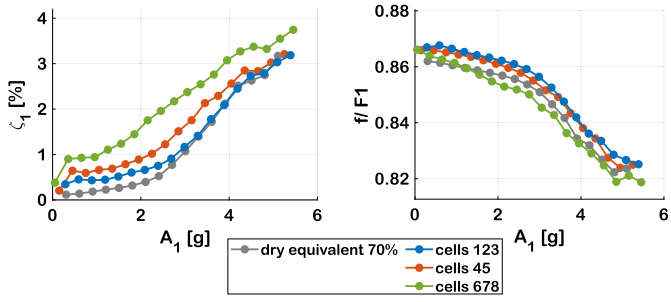


Fig. 12. Damping ratio and frequency versus amplitude for different spanwise positions at 70% filling level.

gray curves), indicating that any induced sloshing damping is not substantial. As the liquid is moved further outboard, the local accelerations increase and the violent vertical sloshing occurs earlier, ultimately starting with the end of the first cycle in cell group 678 (green curves).

There are increasing amounts of damping identified when the sloshing is induced further outboard and this effect is observed throughout the entire amplitude range. The frequencies all vary without major differences within each filling configuration, with only small variation from the reference dry case. These minor differences are likely to be caused by the small differences in the matched mass distributions. It is interesting to note that the frequencies associated with case 678 (green curves) are consistently slightly lower than the other cases and sometimes lower than the dry case in the initial part of the transient (e.g. Figs. 10 and 12). The reason for this phenomenon is that no internal baffles were used and group 678 consists of the three tip cells. Following the initial loading, the liquid is distributed slightly outboard, lowering thus the bending frequency of the sloshing system. In later response stages, the sloshing and structural motion decay, the liquid is distributed more evenly in the spanwise direction, and the frequency approaches the dry value. This effect is most noticeable at the tip of the wing since the largest vertical deflections are also

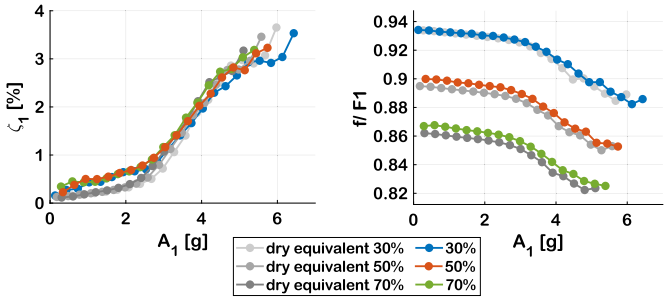


Fig. 13. Damping ratio and frequency versus amplitude for different filling levels and cell group 123.

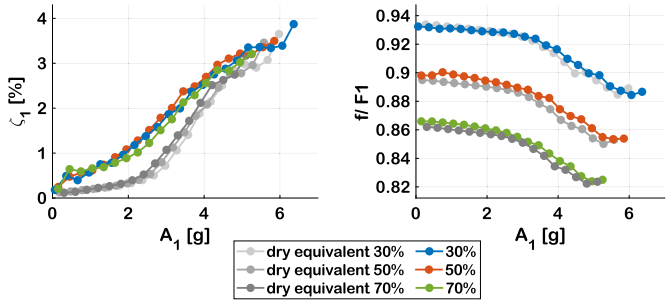


Fig. 14. Damping ratio and frequency versus amplitude for different filling levels and cell group 45.

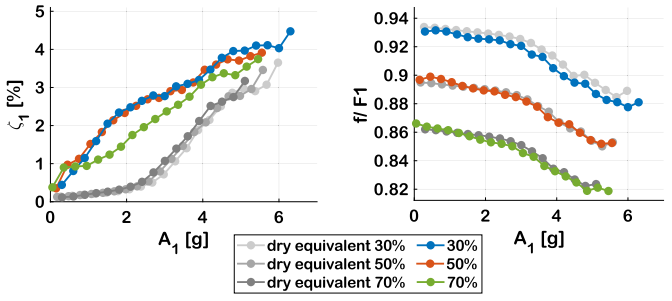


Fig. 15. Damping ratio and frequency versus amplitude for different filling levels and cell group 678.

found there. Overall, as they are observed already in the dry configuration, the identified frequency changes are attributed to the nonlinear structural sources (e.g., freeplay or friction induced softening effects visible mainly at large response amplitudes) which are primarily located at the interface between the demonstrator and the reaction wall.

Figs. 13 to 15 show an alternative way of looking at the same results, namely damping ratio and frequency versus amplitude for different filling levels at the same spanwise positions. The three dry cases with different amounts of added mass are shown, since there are small differences between the identified damping values.

In the previous single-DOF investigations, it was found that the effect of the filling level on the induced or effective damping was substantial - varying the filling level, the damping ratio decreased symmetrically around the 50% filling [8]. In contrast with that observation, in Figs. 13 to 15, it is remarkable that, regardless of the spanwise location, the induced damping effects are much less sensitive to the changes in the filling level in the studied 30-70% range. With the exception of the 70% filling case in cell group 678, Fig. 15, and with a less noticeable effect in group 45, Fig. 14, there is a virtually identical damping evolution indicated by the identified wet damping curves. In fact, the main differences in the 70% fill case may again come from the varying spanwise distribution of the liquid.

Fig. 16 shows video captures at various time instants for cells 678, 70% fill case, taken from the side and top of the tank. Due to the initial deflection of the wing, most of cell 8 is filled completely with liquid. The initial liquid-air boundary is shown in green in the view taken from the top, to better emphasize the spanwise evolution of the sloshing patterns towards the tip of the wing and past the initial boundary between the two phases. Judging by the time evolution of the sloshing patterns in Fig. 16, it can be seen that it takes a substantial amount of time for the liquid to start sloshing at the tip of the wing. As the response amplitude decreases, there is an interplay between the centrifugal forces pushing the liquid towards the tip of the tank during the free vibrations and the natural levelling effect between the three cells due to gravity. The net effect is that the location of the liquid renders cell 8 ineffective from a sloshing point of view, likely being a major effect on the reduction of the damping ratio shown by the green curves in Figs. 14 and 15. The same effect, albeit to a lesser extent, was noticed by inspecting the video footage taken for cells 45 for the 70% fill, but the same is not true for lower filling levels, 30 and 50%, since there is not enough liquid in those cases to fill the outboard cell and thus make it ineffective. While what is observed here in relation to the 70% fill case is still an effect of the filling level, it is of a different nature than the single-DOF cases, due to the bending deformation of the tank and rotation due to the bending of the underlying structure.

One possible reason for the insensitivity of the identified values of damping ratio to the filling level in the wing demonstrator may come from the variation in the bending frequency between the different filling levels. In the previous single-DOF transient cases [8], the frequency of the system was maintained at the constant value between the filling levels, whereas here it changes substantially (see the frequency plots in Figs. 13 to 15). The change in the mass and bending frequency of the system may thus have an effect on the damping ratio between different filling levels.

3.2.4. *Effect of baffles with no dihedral*

The scaled tank is equipped with 7 removable baffles, which allow the investigation of the liquid compartmentalization (as it was shown in Section 3.2.3) and different baffle geometries. There are three cases that will be studied here: the case without the baffles, with the solid-section baffles that seal each cell, and with the slot baffles (see also Fig. 3b for the baffle geometry).

The slot baffles have a 5 mm cut out at their bottom, which allows the liquid to flow between the cells under quasi-static conditions during the static loading, but blocks the flow dynamically, i.e. following the step release. The aim is to restrict the spanwise motion of the liquid during the free decay, but to have the same initial distribution as in the case without baffles. Fig. 17 shows the initial distribution of the liquid for the three cases for 70% filling level. It can be seen that the case with no baffles and with the slot baffles have the same initial liquid configuration. For the case with the solid baffles, each individual cell was filled separately and the three considered filling levels were 30, 50 and 70%.

Figs. 18 to 20 show the damping ratios and frequencies for each filling level, compared to the equivalent dry mass case. In terms of damping ratios, all cases regardless of the baffle configuration show additional dissipation due to sloshing. There is, however, a clear distinction between configuration with the solid baffles and the other two cases. The sloshing-induced damping is substantially higher in the case with the solid baffles.

For instance, an additional damping ratio of 3.66% (0.0366) at $A_1 = 2.55$ g was obtained on top of the dry damping for the 50% fill case with solid baffles. The reason for this difference is fairly

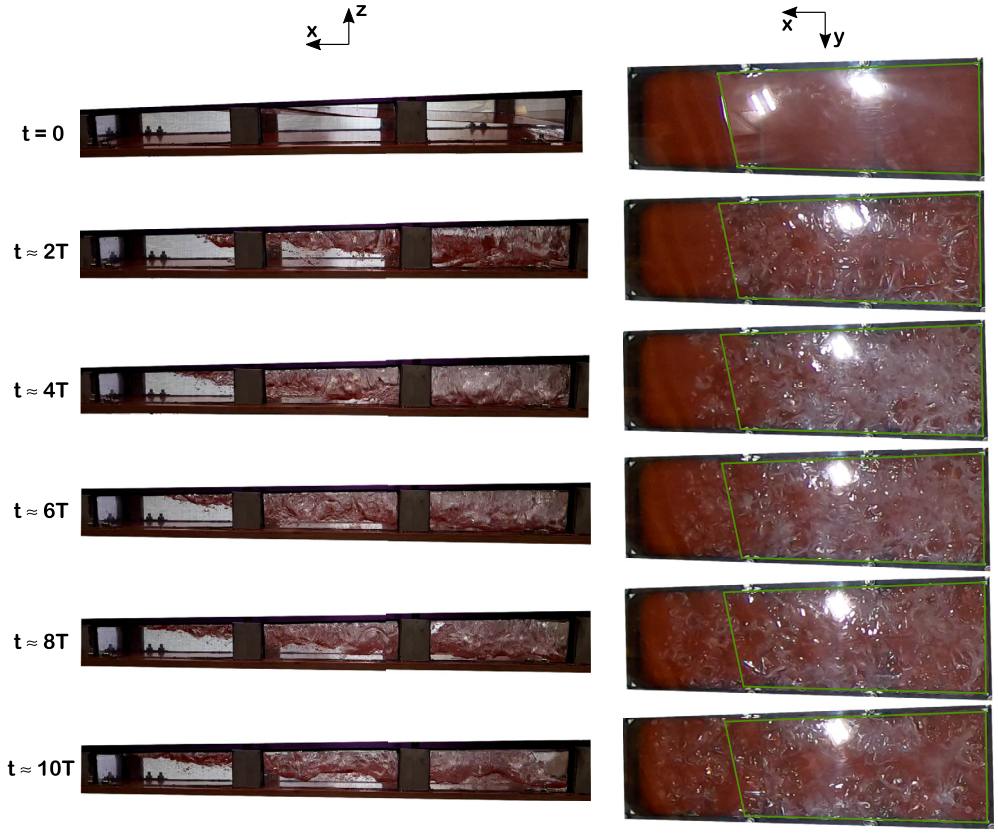


Fig. 16. Snapshots taken from the side and top of the tank showing sloshing progression towards the tip of the wing, cells 678. Pre-release liquid-air boundary shown in green.

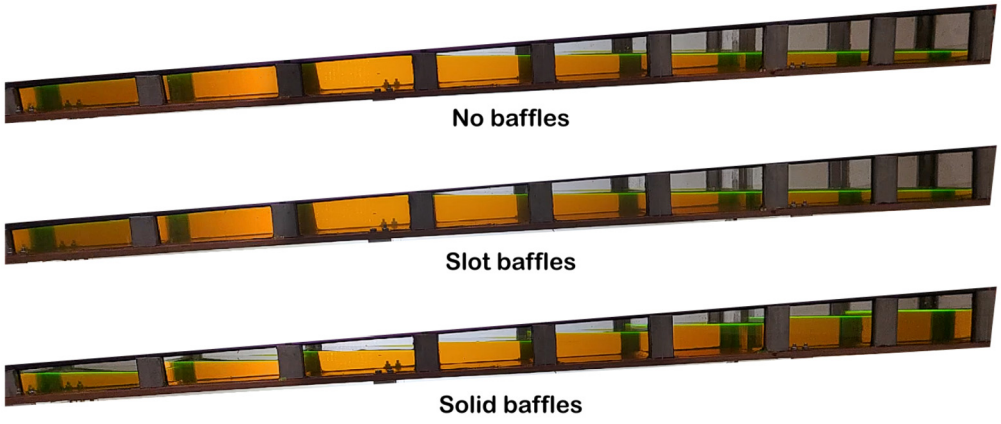


Fig. 17. Example of the initial liquid distribution at $t = 0$ with different baffles.

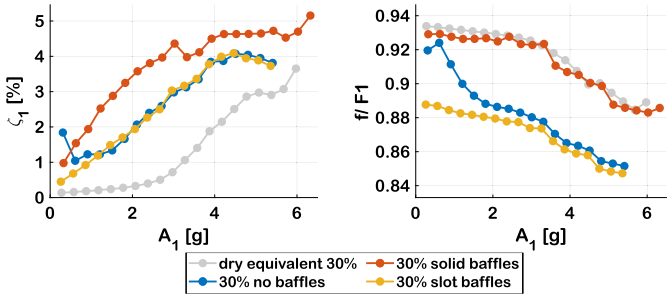


Fig. 18. Damping ratio and frequency versus amplitude for different baffles, 30% fill, $\Lambda = 0°$.

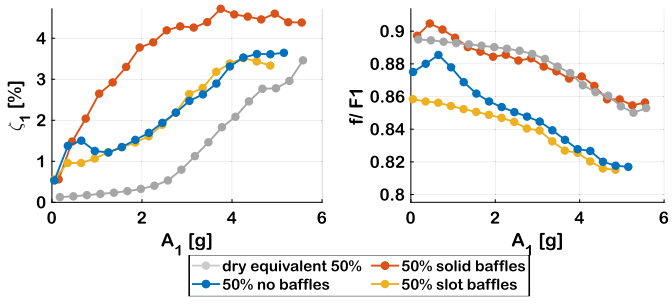


Fig. 19. Damping ratio and frequency versus amplitude for different baffles, 50% fill, $\Lambda = 0°$.

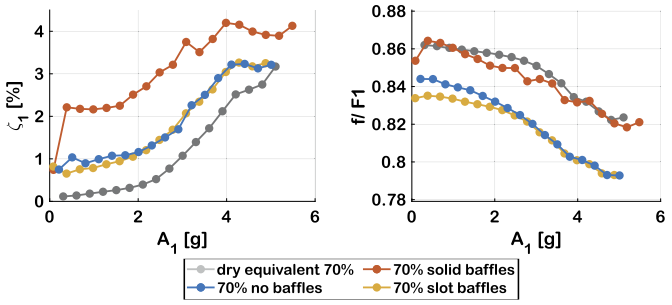


Fig. 20. Damping ratio and frequency versus amplitude for different baffles, 70% fill, $\Lambda = 0°$.

straightforward and can be seen by inspecting again the initial liquid spanwise distribution in Fig. 17. In the case with solid baffles, the liquid is distributed across the entire span, while in the other two, cells 6,7 and 8 are completely flooded initially, being ineffective from a sloshing damping point of view.

The match between the case without and with slot baffles is also noteworthy. The damping curves show substantial overlap which indicates that the induced damping effects are largely unaffected by the spanwise movement of the liquid. Even though in the case without baffles the liquid is allowed to move over the entire span of the tank, its spanwise dynamics is very slow compared to the vertical component which dominates the sloshing damping response. This observation is also supported by studying the frequency curves in Figs. 18 to 20. First of all, when the solid baffles are used the frequencies are higher and closer to the dry case, as the liquid is stopped from moving to the tip of the wing during the static loading phase. For the two other cases, the frequencies are lower and match very well in the initial part of the transient, however, they diverge gradually when moving towards the lower acceleration levels. The reason for this phenomenon is that in the case without baffles (blue curves) the liquid redistributes towards the root following the step release, while the slot baffles do not allow this to happen sufficiently fast. In fact, with slot baffles, the liquid starts to flow from the tip of the tank inboard only after the tank has come to a standstill when A_1 is close to 0 g. There is also a small increase in the damping ratio in the case without baffles at $A_1 < 1$ g, as the liquid that leaves the tip of the tank moves inboard where it contributes to the vertical dissipative motions.

3.2.5. *Effect of dihedral angle: different filling levels*

Civil aircraft wings usually have a nonzero dihedral angle which affects the distribution of the fuel inside the wings under the influence of gravity. With a positive dihedral, the fuel is normally distributed towards the root of the wing, unless special measures are taken to move it to the other parts of the tank or other tanks. Because of the gravitational pull towards the tank root and the different orientation of the tank, the parameters studied before (e.g. filling level or baffle geometry) may influence the induced damping effects in a different manner compared to the case without the dihedral. These aspects make the dihedral angle an important parameter to be considered and bring the experimental analysis closer to a real aircraft configuration.

In the case presented here, the tank with and without perforated baffles is considered, while both cases allow the liquid to move freely between the tank cells. The root wedges of the model were changed such that the dihedral angle was set to 6.9°, the average dihedral of the full-scale reference wing. After changing the root conditions, the modal tests and large amplitude dry tests were redone and no significant changes in the modal properties (e.g. frequencies, mode shapes and damping) were observed. For the filling level study, the case with the scaled baffles (see Fig. 3b) is considered. The scaled baffles have a geometry that is similar to that of the full-scale wing model, and thus this case is the most representative of a commercial aircraft's main wing tank. Filling levels between 10% and 90% with 10% increments are studied.

In order to first gain an appreciation of the liquid distribution at different filling levels when the dihedral is nonzero, Fig. 21 shows the video snapshots taken at $t = 7T$ for all filling levels. The time instance $t = 7T$ was chosen because at this point, for all filling levels, the sloshing patterns (representing vertical liquid-tank impacts at large accelerations and standing waves at small accelerations) were fully developed; note that this aspect is most relevant for the lower fill cases, where the liquid is close to the root, the local vertical accelerations are much lower and consequently the sloshing patterns take longer to fully develop. Multiple interesting particularities can be observed in Fig. 21. First of all, violent vertical motions are apparent regardless of filling level, even in cells 1-3 at the root of the tank for the low liquid fills. The cells of the tank are not uniformly filled and can also contain no liquid at all, or be completely filled. The filling level may also change in time as the liquid moves in the spanwise direction during the transient decay.

Interestingly, part of the effect of the filling level, as opposed to the $\Lambda = 0°$ case, is also to alter the spanwise position of the active sloshing part of the liquid, meaning the amount and location of the liquid that is moving relative to the tank. Table 5 shows which cells are active depending on the filling level, meaning in which cells was the sloshing observed to happen, regardless of its amplitude or sloshing regime.

The liquid mass which moves relative to the tank is expressed as a fraction of the total liquid mass inside the tank. For example, in the 90% fill case, cells 1 to 4 are completely filled with the liquid at all times and the liquid does not move in those cells relative to the tank. Only cells 5 to 8 are thus active and, out of the total liquid mass present in the tank, the mass found in cells 1-4 is not active from a sloshing point of view; the active fraction is thus only 0.42, corresponding to the remaining liquid mass when cells 1-4 are subtracted. From a dynamics point of view, the completely filled cells act as dry mass, still contributing to the modifications in the wing frequencies. Importantly, this table shows that (1) the fraction of the mass which contributes to the energy dissipation changes its spanwise location (shown via the active cells) with the filling level, and (2) the active liquid fraction also varies with the filling level.

Having gained the understanding of the peculiarities of the sloshing patterns and spanwise distribution when the dihedral angle is different from 0°, the dissipative effects are studied next. Fig. 22 shows the damping ratio and frequency versus amplitude for all filling levels and the dry case. Moving from the lower to the higher filling levels, the added damping due to sloshing on top of the dry damping generally increases until it is maximized at the 60% fill, showing less sensitivity around the 40-80% range. Fig. 23 shows alternative views of the damping curves for better overall understanding, including damping vs amplitude and filling level (left), and damping versus filling level (right). The 10% fill curve shows no substantial additional damping due to sloshing. Fig. 21 and Table 5 indicate that even though the entire quantity of liquid undergoes violent vertical motions relative to the tank, the relatively small liquid quantity (only 10% of the tank volume) and its placement in cells 1-3 close to the root leads to negligible sloshing dissipative effects. The cases with 20% and 30% fill show increasing amounts of damping, albeit not in the first few cycles (as seen by the damping ratio curves in Fig. 22 matching the dry curve at the beginning of the transient). More vertical sloshing occurs in cells 4 and 5 for these cases and the entire liquid fraction takes part in the motion, leading to higher damping values compared to the 10% case. Moving to higher filling levels, it is interesting to note that even though not all of the liquid takes part in the sloshing

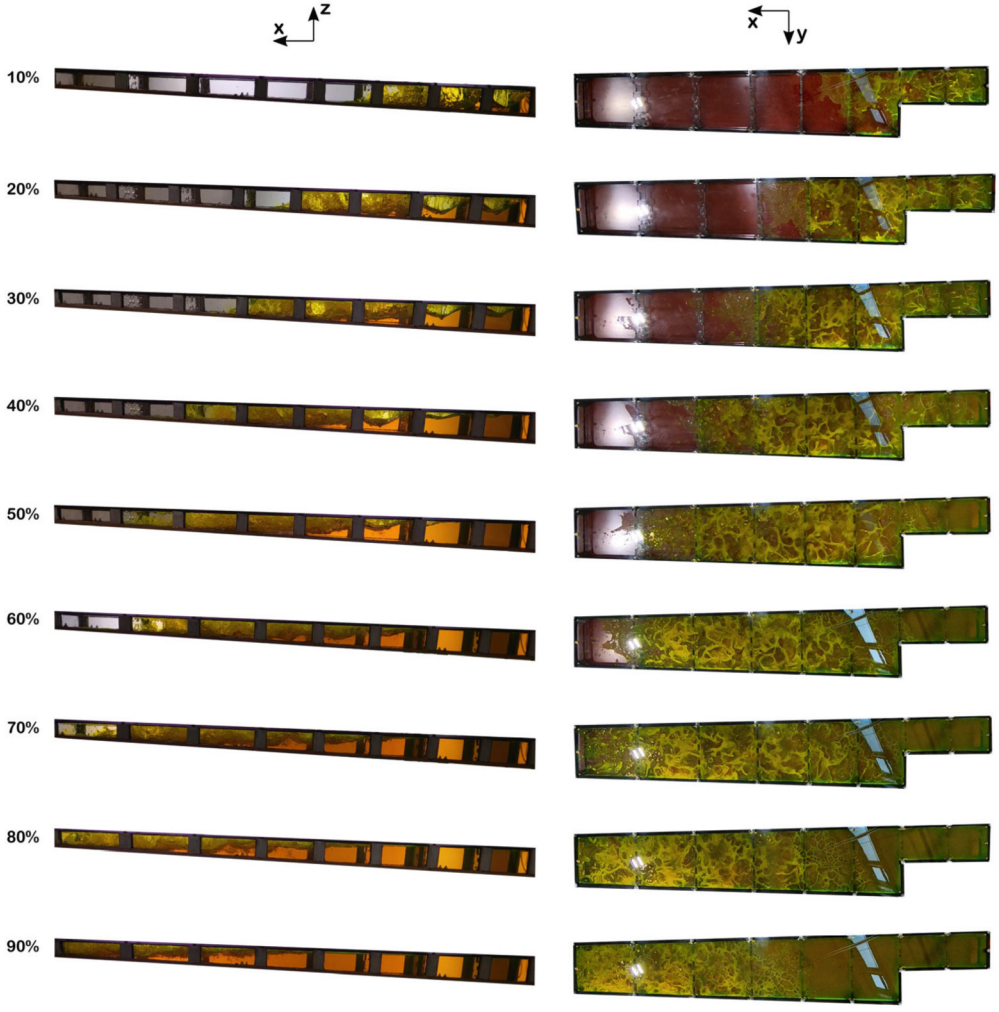


Fig. 21. Snapshots taken from the side and top of the tank for all filling levels, $\Lambda = 6.9°$.

Table 5
Sloshing active cells for each filling level and fraction of liquid which is moving relative to the tank.

Fill [%]	10	20	30	40	50	60	70	80	90
Sloshing active cells	1-3	1-4	1-5	1-6	2-7	3-7	3-8	4-8	5-8
Sloshing active fraction	1	1	1	1	0.81	0.69	0.74	0.55	0.42

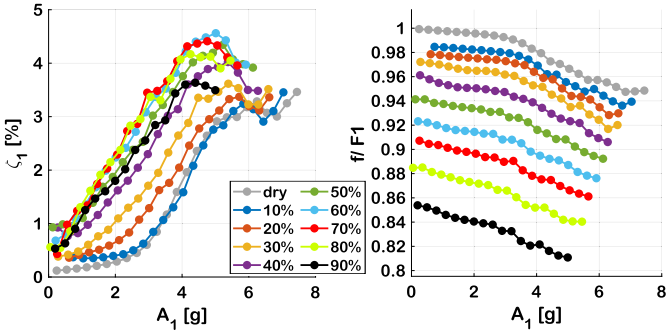


Fig. 22. Damping ratio and frequency versus amplitude for different filling levels, $\Lambda = 6.9°$.

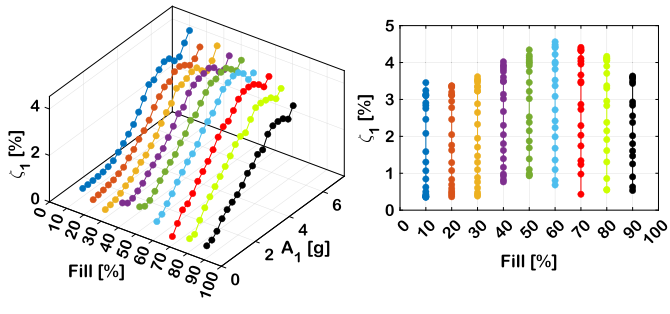


Fig. 23. Damping ratio – amplitude – filling level map, $\Lambda = 6.9°$.

motion (e.g. Table 5 shows that only slightly more than half of the liquid sloshes in the 80% case), this motion is more effective from a damping point of view, as it happens to produce the hydrodynamic forces at the tank interface closer to the tip of the wing. The damping ratio is maximized in the 50-70% fill range, where most of the outboard cells and also a large part of the liquid mass are active. Once the vertical sloshing is developed, an additional 2.33% (0.0233) damping ratio is measured at the 60% fill case on top of the dry damping ratio, at $A_1 = 3.8$ g.

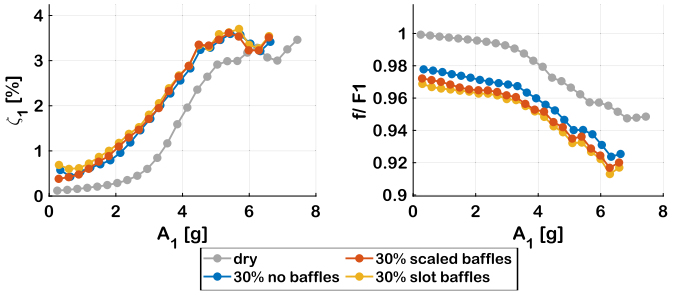


Fig. 24. Damping ratio and frequency versus amplitude for different baffles, 30% fill, $\Lambda = 6.9°$.

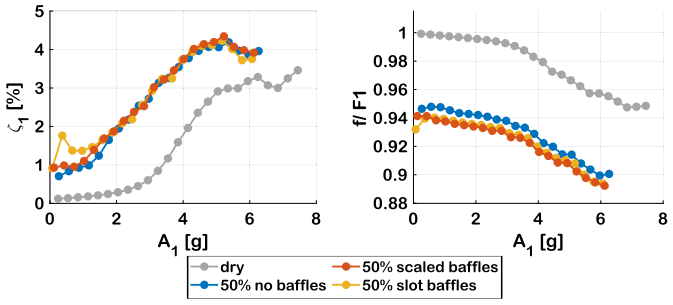


Fig. 25. Damping ratio and frequency versus amplitude for different baffles, 50% fill, $\Lambda = 6.9°$.

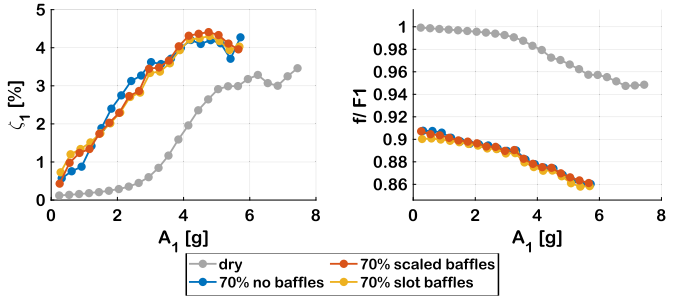


Fig. 26. Damping ratio and frequency versus amplitude for different baffles, 70% fill, $\Lambda = 6.9°$.

3.2.6. *Effect of dihedral: different baffles*

The effect of the baffles on the sloshing-induced dynamics was analysed in Section 3.2.4 for the case without dihedral. Here, the compared tank configurations with the nonzero dihedral angle include the cases without baffles, with the slot baffles and with the scaled baffles (see Fig. 3b). Further, three filling levels are considered, 30%, 50% and 70%.

Figs. 24 to 26 show the damping ratio and frequency versus amplitude for the three baffle cases and three filling levels. The sloshing-induced damping effects are seen for all cases, with virtually no difference caused by the baffles, except for the slight frequency shifts due to the mass distribution. This is significant observation since, when the dihedral angle is $\Lambda = 6.9°$, the spanwise flow restrictions imposed by the baffles do not produce appreciable difference in the identified values of the damping ratio. The case with the realistic baffle geometry (scaled baffles), even though it includes the peculiarities due to the flow through the baffle orifices, is indistinguishable from the point of view of the induced damping effects.

It must be noted that, even though the sloshing-induced damping is not affected by the baffles in this case, some differences in the sloshing patterns are noticeable among the three cases. Fig. 27 shows a series of video captures taken from the top of the tank at different time instances and with the different baffles. Following the step release, the vertical flow first develops close to the walls due to the meniscus and wall shear effects. The presence or absence of the baffles, as well as their geometry, do indeed affects the meniscus and the flow pattern in the initial tank cycle, seen by the flow differences at $t = T$ in Fig. 27. Compared to the baffled cases, even in the second and the third cycle, the absence of the baffles makes the impacts between the liquid and the tank top more noticeable closer to the leading and trailing edges.

As a final note, Fig. 27 reveals the movement of the liquid near the tip of the tank. Following the step release, the liquid starts moving outboard driven by the centrifugal forces, as seen in cell 7 in Fig. 27 for all baffles. This characteristic was observed as well in all other cases that were studied (e.g. with zero dihedral), and here it is particularly noteworthy as there is also an adverse gravitational pull inboard due to the positive dihedral angle.

4. Conclusions

An experimental campaign was conducted to study the impact of fuel sloshing on the vertical dynamics of a scaled wing-fuel tank research demonstrator. The study aimed to examine the impact of excitation amplitude, filling level, baffle geometry, spanwise liquid position, and dihedral angle on the effects of fuel sloshing following a step release excitation.

Sloshing of liquid in the fuel tank causes extra energy dissipation on top of structural damping. The damping depends on filling level and, in the experiments considered, is maximized at 40% fill without dihedral and 60% fill with positive dihedral. The effect also depends on tank orientation and wing bending deflection, unlike in the single-DOF vertical systems [8], higher filling levels can result in parts of the tank being completely filled and thus ineffective from a sloshing point of view. It was also found that the sloshing-induced damping depends on the excitation amplitude in a fashion that is consistent with previous experimental results. Depending on the initial amplitude of the wing, sloshing may take different amounts of time to develop, between half a bending cycle for maximum tank tip accelerations of 6 g, and more than 10 cycles for accelerations lower than 2 g. At large amplitudes of excitation where violent vertical sloshing behaviour is observed, higher damping values are obtained earlier in the transient motion. The strongest impact on net damping comes from the spanwise distribution of liquid, with maximum effects for liquid distribution close to the wing tip.

Three baffle configurations were tested, along with the case without baffles. Baffles mainly impact sloshing-induced damping by compartmentalizing the tank. Solid baffles that maintain a favorable liquid distribution can increase damping, while perforated baffles may not be as effective, as they can allow for sections of the tank to be completely filled with liquid and thus rendering them ineffective. For a 50% filling level with 0° dihedral angle, the use of solid baffles results in an additional 3.66% (0.0366) damping ratio at $A_1 = 2.55$ g, compared to only 1.4% in the case with no baffles. Baffles also alter the sloshing patterns during the first few cycles of motion, linked to meniscus effects with no observed effects on net damping.

The influence of the dihedral angle on the induced damping effects is substantial through its altering of the distribution of the liquid in the spanwise direction under the gravitational effects. Tank baffles have no effect on the damping ratio when the dihedral angle is non-zero, as long as they do not contribute to modifications in the location of the liquid. In this case, the filling level shifts the location and local filling level of the sloshing-active cells, thus affecting the damping ratio. The maximum added damping 2.33% (0.0233) at 60% filling level, regardless of baffles. For com-

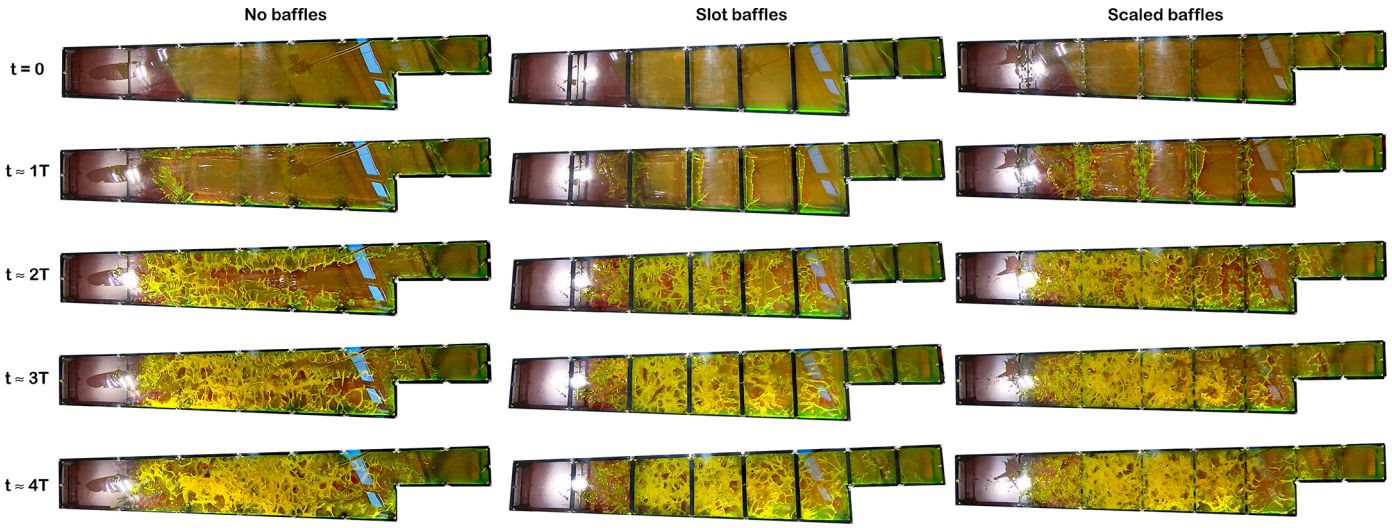


Fig. 27. Snapshots from the top of the tank for the 50% fill and different baffles, $\Lambda = 6.9°$.

parison, a maximum of 3.8% (0.038) added damping was obtained in the case without dihedral (at 40% filling level with solid baffles).

These results are significant as they offer a better understanding of how fuel sloshing may be exploited for increased damping in aircraft wings, especially in correlation with previously-obtained results. Moving the fuel around the different aircraft tanks is already common practice in aiding the trimming of the aircraft. It could be foreseen that by also keeping the fuel compartmentalized preferentially in the 40-60% filling level in optimally chosen positions, depending on availability during flight, may improve the gust response of the wing in a predictable manner. However, further work that builds upon the results presented here is needed.

Declaration of competing interest

The authors declare the following financial interests/personal relationships which may be considered as potential competing interests: Jonathan E. Cooper reports financial support was provided by Horizon 2020, grant agreement No. 815044.

Data availability

Data will be made available on request.

Acknowledgement

The research leading to these results was undertaken as part of the SLOWD project which has received funding from the European Union's Horizon 2020 research and innovation programme under grant agreement No. 815044.

References

[1] R. Langton, C. Clark, M. Hewitt, L. Richards, Aircraft Fuel Systems, John Wiley & Sons, Ltd, 2009, pp. 301–303, Ch. 12.4.
[2] F. Gambioli, et al., Sloshing wing dynamics – project overview, in: Proceedings of 8th Transport Research Arena TRA, Helsinki, Finland, 2020.
[3] EASA, Certification Specifications and Acceptable Means of Compliance for Large Aeroplanes (CS-25) Amendment 27, Tech. Rep. AMC 25.341 Gust and Continuous Turbulence Design Criteria, Section 6 – Aeroplane modelling considerations, European Union Safety Aviation Agency (EASA), 24 November 2021.
[4] B. Titurus, J. Cooper, F. Saltari, F. Mastroddi, F. Gambioli, Analysis of a sloshing beam experiment, in: International Forum on Aeroelasticity and Structural Dynamics, vol. 139, Savannah, Georgia, U.S., 2019.
[5] F. Gambioli, R. Usach, J. Kirby, T. Wilson, P. Behruzi, Experimental evaluation of wing sloshing effects on wing dynamics, in: International Forum on Aeroelasticity and Structural Dynamics, vol. 139, Savannah, Georgia, U.S., 2019.
[6] K. Kotsarinis, M. Green, A. Simonini, O. Debarre, T. Magin, A. Tafuni, Modeling sloshing damping for spacecraft: a smoothed particle hydrodynamics application, Aerosp. Sci. Technol. 133 (2023) 108090, https://doi.org/10.1016/j.ast.2022.108090.
[7] J. Liu, Y. Li, W. Li, B. Zhuang, C. Zhou, Experimental investigation of liquid transport in a vane type tank of satellite with microgravity, Aerosp. Sci. Technol. 105 (2020) 106007, https://doi.org/10.1016/j.ast.2020.106007.
[8] L. Constantin, J. De Courcy, B. Titurus, T. Rendall, J. Cooper, Analysis of damping from vertical sloshing in a sdof system, Mech. Syst. Signal Process. 152 (2021) 107452, https://doi.org/10.1016/j.ymssp.2020.107452.
[9] L. Constantin, J. De Courcy, B. Titurus, T. Rendall, J. Cooper, Sloshing induced damping across Froude numbers in a harmonically vertically excited system, J. Sound Vib. 510 (2021) 116302, https://doi.org/10.1016/j.jsv.2021.116302.
[10] L. Constantin, J. De Courcy, B. Titurus, T. Rendall, J. Cooper, Nonlinear damping effects in vertically vibrating systems with violently sloshing liquid, J. Sound Vib. (2022) 117405, https://doi.org/10.1016/j.jsv.2022.117405.
[11] F. Saltari, M. Pizzoli, G. Coppotelli, F. Gambioli, J.E. Cooper, F. Mastroddi, Experimental characterisation of sloshing tank dissipative behaviour in vertical harmonic excitation, J. Fluids Struct. 109 (2022) 103478, https://doi.org/10.1016/j.jfluidstructs.2021.103478.
[12] J.J. De Courcy, L. Constantin, B. Titurus, T. Rendall, J.E. Cooper, Gust loads alleviation using sloshing fuel, in: AIAA Scitech 2021 Forum, 2021, https://doi.org/10.2514/6.2021-1152.
[13] F. Saltari, M. Pizzoli, F. Gambioli, C. Jetzschmann, F. Mastroddi, Sloshing reduced-order model based on neural networks for aeroelastic analyses, Aerosp. Sci. Technol. 127 (2022) 107708, https://doi.org/10.1016/j.ast.2022.107708.
[14] C.C. Smith Jr., The effects of fuel sloshing on the lateral stability of a free-flying airplane model, Tech. Rep., University of North Texas Libraries, UNT Libraries Government Documents Department, 1948.
[15] E.W. Graham, The forces produced by fuel oscillation in a rectangular tank, Tech. Rep., Douglas Aircraft Company Inc., Santa Monica, California, U.S., 1951.
[16] E.W. Graham, A. Rodriguez, The characteristics of fuel motion which affect airplane dynamics, Tech. Rep., Douglas Aircraft Company Inc., Santa Monica, California, U.S., 1952.
[17] A.A. Schy, A theoretical analysis of the effects of fuel motion on airplane dynamics, Tech. Rep., National Advisory Committee for Aeronautics, 1951.
[18] H. Luskin, E. Lapin, An analytical approach to the fuel sloshing and buffeting problems of aircraft, J. Aeronaut. Sci. 19 (4) (1952) 217–228.
[19] K.F. Merten, B.H. Stephenson, Some dynamic effects of fuel motion in simplified model tip tanks on suddenly excited bending oscillations, Tech. Rep., University of North Texas Libraries, UNT Libraries Government Documents Department, 1952.
[20] E. Widmayer, J.R. Reese, Moment of inertia and damping of fluid in tanks undergoing pitching oscillations, Tech. Rep., National Advisory Committee for Aeronautics, 1953.
[21] J.R. Reese, J.L. Sewall, Effective moment of inertia of fluid in offset, inclined, and swept-wing tanks undergoing pitching oscillations, Tech. Rep., National Advisory Committee for Aeronautics, 1955.
[22] J.R. Reese, Some effects of fluid in pylon-mounted tanks on flutter, Tech. Rep., University of North Texas Libraries, UNT Libraries Government Documents Department, 1955.
[23] J.L. Sewall, An experimental and theoretical study of the effect of fuel on pitching-translation flutter, Tech. Rep., National Advisory Committee for Aeronautics, 1957.

[24] W.H. Gayman, An investigation of the effect of a varying tip-weight distribution on the flutter characteristics of a straight wing, J. Aeronaut. Sci. 19 (5) (1952) 289–301, https://doi.org/10.2514/8.2271.
[25] J.L. Sewall, R.W. Herr, W.B. Igoe, Flutter investigation of a true-speed dynamic model with various tip-tank configurations, Tech. Rep., National Advisory Committee for Aeronautics, 1955.
[26] Vertol Division, The Boeing Company, Wind tunnel tests and further analysis of the floating wing fuel tanks for helicopter range extension. Volumes 1-5, Tech. Rep., The Boeing Company, 1961.
[27] J. Hall, T. Rendall, C. Allen, H. Peel, A multi-physics computational model of fuel sloshing effects on aeroelastic behaviour, J. Fluids Struct. 56 (2015) 11–32, https://doi.org/10.1016/j.jfluidstructs.2015.04.003.
[28] C. Farhat, E. Chiu, D. Amsallem, J. Schotté, R. Ohayon, Modeling of fuel sloshing and its physical effects on flutter, AIAA J. 51 (9) (2013) 2252–2265, https://doi.org/10.2514/1.J052299.
[29] R.D. Firouz-Abadi, P. Zarifian, H. Haddadpour, Effect of fuel sloshing in the external tank on the flutter of subsonic wings, J. Aerosp. Eng. 27 (5) (2014) 04014021, https://doi.org/10.1061/(ASCE)AS.1943-5525.0000261.
[30] L. Constantin, J. De Courcy, B. Titurus, T. Rendall, J.E. Cooper, Design and GVT of a dynamically scaled wing structure for fuel sloshing investigations, in: AIAA SCITECH 2022 Forum, San Diego, CA & Virtual, AIAA, 2022, https://doi.org/10.2514/6.2022-2133.
[31] R. Bass, E. Bowles Jr., R. Trudell, J. Navickas, J. Peck, N. Yoshimura, S. Endo, B. Pots, Modeling criteria for scaled LNG sloshing experiments, Trans. ASME J. Fluids Eng. 107 (273) (1985), https://doi.org/10.1115/1.3242473.
[32] R. Bisplinghoff, Aeroelasticity, first Dover ed., Dover Publications, 1996, Ch. 12.
[33] J.R. Wright, J.E. Cooper, Introduction to Aircraft Aeroelasticity and Loads, John Wiley & Sons, Ltd, 2014, pp. 301–303, Ch. 14.
[34] J.R. Fuller, Evolution of airplane gust loads design requirements, J. Aircr. 32 (2) (1995) 235–246, https://doi.org/10.2514/3.46709.
[35] C.P. Szczyglowski, S.A. Neild, B. Titurus, J.Z. Jiang, E. Coetzee, Passive gust loads alleviation in a truss-braced wing using an inerter-based device, J. Aircr. 56 (6) (2019) 2260–2271, https://doi.org/10.2514/1.C035452.
[36] A. Fellowes, T. Wilson, G. Kemble, C. Havill, J. Wright, Wing box non-linear structural damping, in: International Forum on Aeroelasticity and Structural Dynamics, Paris, France, 2011.
[37] J. Calderon-Sanchez, J. Martinez-Carrascal, L.M. Gonzalez-Gutierrez, A. Colagrossi, A global analysis of a coupled violent vertical sloshing problem using an SPH methodology, Eng. Appl. Comput. Fluid Mech. 15 (1) (2021) 865–888, https://doi.org/10.1080/19942060.2021.1921849.
[38] L. International, The LMS Test.Lab Modal Analysis Manual, Rev 12A, Siemens, 2012.
[39] L. Constantin, J.J. De Courcy, B. Titurus, T.C.S. Rendall, J.E. Cooper, F. Gambioli, Effect of fuel sloshing on the damping of a scaled wing model: experimental testing and numerical simulations, Appl. Sci. 12 (15) (2022), https://doi.org/10.3390/app12157860.
[40] M. Alam, M. Hromcik, T. Hanis, Active gust load alleviation system for flexible aircraft: mixed feedforward/feedback approach, Aerosp. Sci. Technol. 41 (2015) 122–133, https://doi.org/10.1016/j.ast.2014.12.020.
[41] R. Langton, C. Clark, M. Hewitt, L. Richards, Fuel System Design Examples, John Wiley & Sons, Ltd, 2009, pp. 271–325, Ch. 12.